Mon. Not. R. Astron. Soc. **347,** L47–L51 (2004)

On the power-law tail in the mass function of protostellar condensations and stars

Shantanu Basu★ and C. E. Jones
Department of Physics and Astronomy, University of Western Ontario, London, Ontario, Canada N6A 3K7

Accepted 2003 November 7. Received 2003 November 4; in original form 2003 September 24

ABSTRACT

We explore the idea that the power-law tail in the mass function of protostellar condensations and stars arises from the accretion of ambient cloud material on to a condensation, coupled with a non-uniform (exponential) distribution of accretion lifetimes. This model allows for the generation of power-law distributions in all star-forming regions, even if condensations start with a lognormal mass distribution, as may be expected from the central limit theorem, and supported by some recent numerical simulations of turbulent molecular clouds. For a condensation mass m with growth rate $\mathrm{d}m/\mathrm{d}t \propto m$, an analytic three-parameter probability density function is derived; it resembles a lognormal at low mass and has a pure power-law high-mass tail. An approximate power-law tail is also expected for other growth laws, and we calculate the distribution for the plausible case $\mathrm{d}m/\mathrm{d}t \propto m^{2/3}$. Furthermore, any single time snapshot of the masses of condensations that are still accreting (and are of varying ages) also yields a distribution with a power-law tail similar to that of the initial mass function.

Key words: accretion, accretion discs – stars: formation – stars: luminosity function, mass function – ISM: clouds.

1 INTRODUCTION

1.1 Initial mass function background

Despite decades of detailed modelling of gravitational collapse and fragmentation, it is still not clear how certain physical conditions determine the mass of an individual star; a larger question is the origin of the *distribution* of stellar masses at birth, the stellar initial mass function (IMF). Additionally, the observed mass spectrum of protostellar condensations in molecular clouds appears to follow a power-law decrease, similar to that of stars, in the mass range above $\sim$0.5 $\mathrm{M}_{\odot}$ (Motte, André & Neri 1998; Testi & Sargent 1998; Johnstone et al. 2000). Hence the fundamental shape of the IMF may be determined at the molecular fragment scale, even though the transformation of a condensation to star(s) is not a simple process.

Starting with the expression for the Jeans (1928) mass, and working up to more sophisticated scenarios, there is a general tendency for multiplicative dependence on physical parameters (see e.g. Adams & Fatuzzo 1996), leading to the claim that the central limit theorem should ensure that the IMF has a lognormal form. The formation of star-forming condensations in a molecular cloud is surely affected by multiple effects of a turbulent flow field, and statistical variations of ambient magnetic field, density, pressure and temperature. Numerical models of turbulent molecular clouds typically yield a lognormal distribution of dense clump masses (e.g. Padoan, Nordlund & Jones 1997; Ostriker, Stone & Gammie 2001; Klessen 2001). Although much additional physics remains to be included in these models, it may be reasonable to believe that the stochastic feature of a lognormal distribution will continue to hold. Hence one can ask a simple set of questions about star formation: Is the IMF lognormal? If not, and an approximate power-law tail is inferred, then how is it generated?

While Miller & Scalo (1979) did obtain a lognormal fit to the IMF, subsequent detailed studies find a region of power-law decrease in the intermediate- and high-mass (M) range that is similar to the original result of Salpeter (1955), i.e. $\mathrm{d}N/\mathrm{d}\ln M \propto M^{-1.35}$, where $\mathrm{d}N$ is the differential number of stars in the logarithmic mass interval $\mathrm{d}\ln M$ (see e.g. reviews by Scalo 1998; Meyer et al. 2000; Elmegreen 2001). Scalo (1998) emphasizes a varying power-law index in the intermediate- and high-mass range, with significant region-to-region variations reflecting intrinsic variability and/or observational uncertainties.

1.2 Lognormal or power-law distribution?

The generation processes of lognormal and power-law distributions are often intimately connected. This phenomenon has been studied extensively in social science, biology and computer science, e.g. in the study of power-law distributions of income (the Pareto Law), city sizes (Zipf's Law), and Internet file sizes. Useful models and discussion can be found in Reed (2002, 2003), Reed & Hughes

★E-mail: basu@astro.uwo.ca

(2002), Mitzenmacher (2004), and references within. It turns out that many seemingly small effects in the generative process of a lognormal distribution can lead to a power-law tail instead. Such an explanation seems particularly relevant for the IMF, since the power-law tail is typically measured to span even less than two decades of mass, hardly qualifying as evidence for a truly scale-free process.

In this Letter, we propose a minimum-hypothesis explanation: even if the central limit theorem is relevant in determining the starting masses of condensations, the temporal effect of their subsequent interaction with the environment skews the mass distribution into a power-law form. This paper is based on the statistical model summarized by Reed & Hughes (2002), and builds upon some elements of the model of Myers (2000). The basic idea is that the growth of masses by accretion coupled with a *distribution of times* for the growth yields a power-law tail in the mass function. It is a statistical approach, not dependent on the detailed values of physical variables in different environments. While the mass of any individual star is dependent on the particular initial values of various physical parameters, we are concerned here only with the *shape* of the mass distribution function; specifically the intermediate- and high-mass tail.

2 LOGNORMAL FITS AND POWER-LAW TAIL IN THE IMF: A CASE STUDY

In order to establish the minimum requirements for an IMF model, we review the data from the Orion Nebula Cluster (ONC) obtained by Hillenbrand (1997, hereafter H97). The ONC is a unique laboratory for the study of the IMF because of its relatively nearby location and direction away from the Galactic plane, allowing a deep sampling of the young stellar population in the vicinity of the massive star θ^1C. The large range of surface density from centre to observed edge of the cluster, and the large number of observed stars, allows for useful statistics on the role of the environment (specifically the density of stars) in the generation of the IMF. Furthermore, since most stars have estimated ages less than a few Myr (H97), they are probably observed near their birth sites. The IMF of H97 also shows a decline at lower masses, which we utilize to assess the viability of lognormal fits.

Fig. 1 shows the distribution of 696 stellar masses obtained by H97; these are the subset of observed stars that are reported to have a 70 per cent or higher chance of membership in the ONC. We do not try to account for uncertainties in the mass determinations here, and simply seek a best-fitting lognormal probability density function

$$f(m) = \frac{1}{\sqrt{2\pi}\sigma m} \exp\left[-\frac{(\ln m - \mu)^2}{2\sigma^2}\right] \quad (1)$$

for the normalized masses $m = M/\mathrm{M}_\odot$. For comparison with a sample of $N_{\rm tot}$ objects, the normalized number in each bin, $\mathrm{d}N/N_{\rm tot}$, equals $f(m)\ \mathrm{d}m = mf(m)\ \mathrm{d}\ln m$, where $\mathrm{d}\ln m$ is the width of a logarithmic mass bin. We conduct a parameter search of values of the mean μ and variance σ^2 of $\ln\ m$. Minimization of the χ^2 deviation of the observed values from the analytic curves yields best-fitting parameters $\mu = -1.08$ and $\sigma = 1.16$. The dash–dotted line in Fig. 1 is a lognormal distribution with these parameters. Clearly, the ability to fit the tail of the distribution is inconsistent with fitting the peak at the low-mass end. The reduced χ^2 for this fit is $\chi^2_{\rm r} = \chi^2/\nu = 6.64$ for $\nu = 12$ degrees of freedom, yielding a probability 4.75×10^{-12} that the data are drawn from the lognormal distribution. Alternatively, we may seek the best-fitting lognormal to a subset of the data; fitting only stars in bins centred at $M < 1\ \mathrm{M}_\odot$ yields best parameters $\mu = -1.40$ and $\sigma = 0.52$. Fig. 1 also shows this fit (dashed line), which has $\chi^2_{\rm r} = 1.86$ and $\nu = 3$, yielding a probability of 0.134 that the data are drawn from the distribution. A conclusion is that the IMF can be approximately fitted by a lognormal at low mass, but has a power-law intermediate- and high-mass tail. The histogram yields a least-squares best-fitting straight line of slope $\Gamma = \mathrm{d}\log\ N/\mathrm{d}\log M = -1.13$ for $M \geqslant 1\ \mathrm{M}_\odot$.

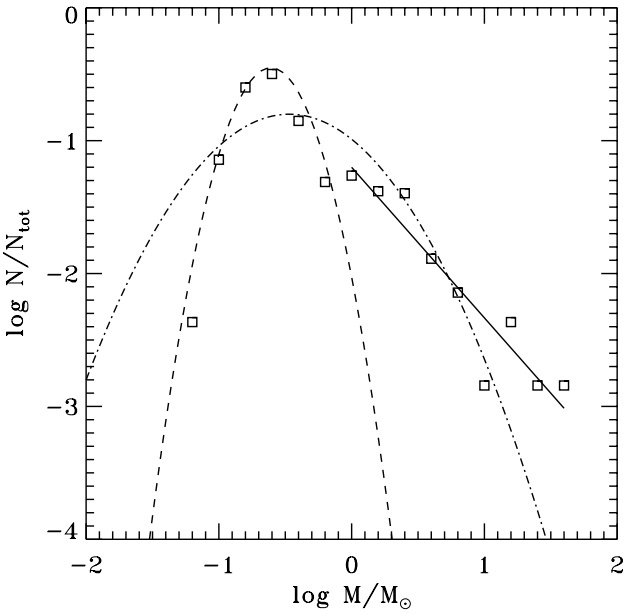

Figure 1. Estimated stellar masses in the ONC and best-fitting analytic curves. The squares represent the masses estimated by H97, binned in intervals $\Delta\ \log\ (M/\mathrm{M}_\odot) = 0.2$. The dashed line is the best-fitting lognormal distribution (equation 1, with $\mu = -1.40$, $\sigma = 0.52$) for $M < 1\ \mathrm{M}_\odot$; the dash–dotted line is the best-fitting lognormal distribution ($\mu = -1.08$, $\sigma = 1.16$) for all masses. The solid line is the least-squares best-fitting straight line for the region $M \geqslant 1\ \mathrm{M}_\odot$; it has slope $\Gamma = \mathrm{d}\log\ N/\mathrm{d}\log\ M = -1.13 \pm 0.15$.

Because of the large variation in stellar surface density in the ONC, we also look for systematic location-dependent effects on the IMF by dividing the stars into three radial zones, each containing about 232 stars, enough for a meaningful statistical sample. Table 1 lists the values of $\chi^2_{\rm r}$ from comparing the histogram of masses $M < 1\ \mathrm{M}_\odot$ in each zone with the best-fitting lognormal for all zones: $\mu = -1.40$, $\sigma = 0.52$. The implied probabilities range from 0.287 to 0.616. For $M \geqslant 1\ \mathrm{M}_\odot$, the best-fitting slopes to the power-law tail are shallower than -1 in radial zones 1 and 2, although there are significant uncertainties in the fits. Interestingly, if we exclude the (merely five) stars in bins centred at $M > 10\ \mathrm{M}_\odot$, all slopes become somewhat steeper than -1. Four of the five excluded stars are in zone 1 (these are the Trapezium stars) and one is in zone 2.

The ONC data imply a generation of essentially the same power law in *all* regions, despite large differences in stellar density (see Table 1). The five most massive stars, four of which are very near the core of the ONC, provide the only significant evidence for a region-dependent IMF. Their presence and location may be due to events occurring after star formation, since the local relaxation time decreases toward the cluster centre as a result of increasing density. However, the simulations of dynamical mass segregation by Bonnell & Davies (1998) imply that they could not have formed very far from the cluster centre. In any case, we bypass the nagging questions about the origin of these five stars, and focus instead on

Table 1. Summary of best-fitting parameters.

Zone	Surface density (pc^{-2})	$M < 1\ M_\odot$ lognormal χ^2_r	$M < 1\ M_\odot$ probability	$M \geqslant 1\ M_\odot$ best slope	$1 \leqslant M \leqslant 10\ M_\odot$ best slope
All ($0 \leqslant r < 17.70$ pc)	0.71	1.86	0.134	-1.13 ± 0.15	-1.53 ± 0.27
1 ($0 \leqslant r < 4.32$ pc)	3.94	0.598	0.616	-0.85 ± 0.21	-1.36 ± 0.39
2 ($4.32 \leqslant r < 8.65$ pc)	1.32	1.25	0.287	-0.89 ± 0.16	-1.12 ± 0.22
3 ($8.65 \leqslant r < 17.70$ pc)	0.31	1.17	0.318	-1.10 ± 0.45	-1.10 ± 0.45

an explanation for the generation of a universal power-law tail in the mass function of all other stars.

3 A STATISTICAL MODEL OF GROWTH BY ACCRETION

3.1 Basic model

According to the central limit theorem of statistics, if the mass of a protostellar condensation $M_c = f_1 \times f_2 \times \cdots \times f_N$, then the distribution of M_c tends to a lognormal regardless of the distributions of the individual physical parameters f_i ($i = 1, \ldots, N$), if N is large. Depending on the specific distributions of the f_i, a convergence to a lognormal may even occur for moderate N (Ioka & Nakamura 2002). However, the stellar IMF results from further evolution beyond the condensation phase, so that the mass of a star may be characterized as $M_s = M_c \times f_{frag} \times f_{out}$, where f_{frag} is the fraction of the condensation mass that goes into a star after any possible fragmentation process, and f_{out} is the fraction of mass that remains after mass loss due to a protostellar outflow. The multiplicative nature of these processes seems consistent with theoretical models (Shu et al. 1999; Meyer et al. 2000), and implies that the distribution of M_s should be lognormal if that of M_c is lognormal as well.

Here we explore the idea that the power-law tail is due to the interaction of a condensation with its environment in the time before it collapses down to stellar dimensions. The environment of a condensation is certainly a large reservoir of mass, and there may be dynamical influences due to the passage of ambient pressure fluctuations, including shocks. If the accretion is a continuous time multiplicative process,

$$\frac{dm}{dt} = \gamma m \Rightarrow m(t) = m_0 \exp(\gamma t), \tag{2}$$

where γ is a growth rate and m_0 is an initial mass. If the values of m_0 are drawn from a lognormal distribution with mean μ_0 and variance σ_0^2, the distribution of masses $f(m)$ at any later time t will still be described by equation (1), but with

$$\mu = \mu_0 + \gamma t, \quad \sigma = \sigma_0. \tag{3}$$

However, all condensations may not accrete for the same time period, and a distribution of accretion times t will in fact skew the final distribution away from a lognormal. A simple example of a distribution of times is if the probability of stopping accretion is constant in time. A constant 'death' rate δ for accretion leads to an exponential distribution, with probability density function $f(t) = \delta\, e^{-\delta t}$. In this case, the probability density function for masses is

$$f(m) = \int_0^\infty \frac{\delta e^{-\delta t}}{\sqrt{2\pi}\sigma_0 m} \exp\left[-\frac{(\ln m - \mu_0 - \gamma t)^2}{2\sigma_0^2}\right] dt. \tag{4}$$

Using the integral identity

$$\int_0^\infty \exp[-(ax^2 + bx + c)]\, dx = \frac{1}{2}\sqrt{\frac{\pi}{a}} \exp[(b^2 - 4ac)/4a] \mathrm{erfc}\left(\frac{b}{2\sqrt{a}}\right), \tag{5}$$

in which

$$\mathrm{erfc}(x) = \frac{2}{\sqrt{\pi}} \int_x^\infty \exp(-u^2)\, du \tag{6}$$

is the complementary error function, we find

$$f(m) = \frac{\alpha}{2} \exp\left[\alpha\mu_0 + \alpha^2\sigma_0^2/2\right] m^{-1-\alpha} \times \mathrm{erfc}\left[\frac{1}{\sqrt{2}}\left(\alpha\sigma_0 - \frac{\ln m - \mu_0}{\sigma_0}\right)\right], \tag{7}$$

where $\alpha = \delta/\gamma$ is the dimensionless ratio of 'death' rate to 'growth' rate of condensations. Equation (7) represents a new three-parameter (μ_0, σ_0, α) probability density function which tends to the form $m^{-1-\alpha}$ for large masses, but is modulated by the complementary error function (which goes to 0 for very low m and to 2 for large m) so that it tends toward zero at very low masses. It is therefore similar to a lognormal distribution with a power-law tail. [Note that it reduces to a pure power-law distribution if all stars start with the same mass m_i, i.e. m_0 is described by a delta function, so that $\mu_0 = \ln\ m_i$ and $\sigma_0 = 0$ in equation (7).] We believe that this function can be used fruitfully to model the IMF.

Physically, we expect $\alpha \approx 1$ since both δ and γ are rates controlled by the external medium and are expected to be approximately the inverse external dynamical time $t_d^{-1} = (G\rho_{ext})^{1/2}$, in which ρ_{ext} is the mean density outside the condensation. Myers (2000) has derived an example of exponential growth with $\gamma \approx t_d^{-1}$, assuming geometric accretion (see equation 9) and that every condensation increases its internal turbulence continuously (as the mass increases) exactly as needed to remain in a critical Bonnor–Ebert state.

Fig. 2 shows a sample initial lognormal distribution ($\mu_0 = -1.40$, $\sigma_0 = 0.52$), and a distribution at a later time under the assumptions (1) multiplicative growth (equation 2) in which all condensations accrete for a fixed time $t = \gamma^{-1}$, and (2) multiplicative growth with an exponential distribution of times $f(t) = \delta\, e^{-\delta t}$. Under assumption (1), the new distribution is again a lognormal with $\mu = \mu_0 + 1$, but in case (2) it is given by equation (7) and has a power-law tail with index $\alpha = 1$ if $\delta = \gamma$.

Recently, Reed (2002, 2003) has derived a probability density function that is even more general than equation (7). It assumes the growth law known as geometric Brownian motion: $dm/m = \gamma\, dt + \sigma_1\, dw$, where dw is a 'white-noise' random number drawn uniformly from the range [0, 1]. In this case, an initially lognormal distribution characterized by μ_0 and σ_0 also remains lognormal after a fixed time t, but with variance $\sigma^2 = \sigma_0^2 + \sigma_1^2 t$, and mean $\mu = \mu_0 + (\gamma - \sigma_1^2/2)t$.

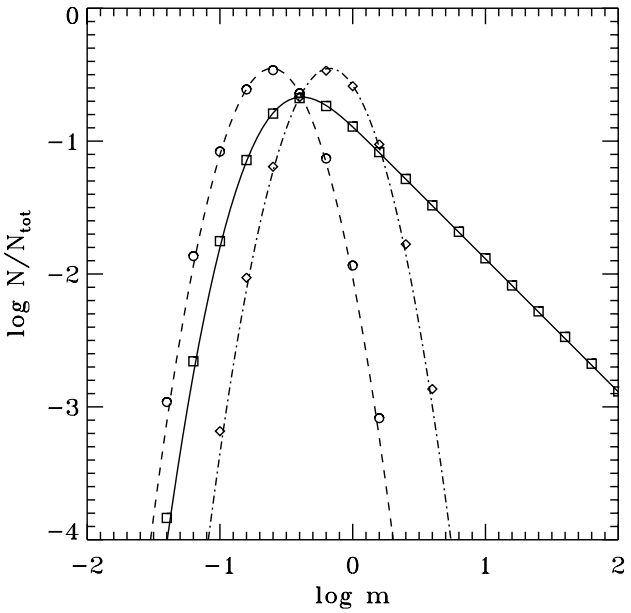

Figure 2. Evolution of a distribution of normalized masses m undergoing accretion growth $\mathrm{d}m/\mathrm{d}t \propto m$ (equation 2). The dashed line is an example of an initial lognormal distribution with $\mu_0 = -1.40, \sigma_0 = 0.52$, and the circles represent a histogram (binned with $\Delta\log\ m = 0.2$) of a random sample of 10^6 objects drawn from the distribution. The dash–dotted line is the analytic expression for the distribution [equation (1) with $\mu = \mu_0 + 1$] if the masses grow for a fixed time $t = \gamma^{-1}$. The solid line is the analytic density function [equation (7) with $\mu_0 = -1.40$, $\sigma_0 = 0.52$, $\alpha = 1$] if accretion lifetimes have density function $f(t) = \delta\ \mathrm{e}^{-\delta t}$, and $\delta = \gamma$. The diamonds and squares represent the histogram of the masses in the original distribution if they grow for a fixed time or with an exponential distribution of times, respectively; they necessarily overlap the analytically predicted curves.

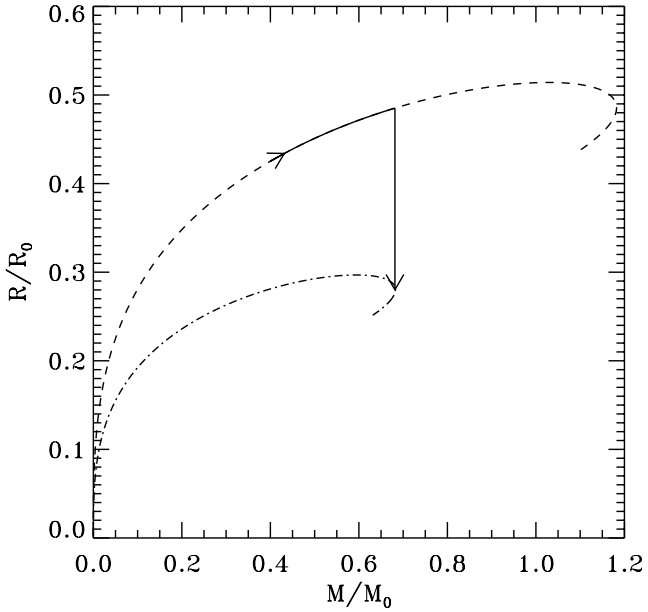

Figure 3. Radius (R/R_0) versus mass (M/M_0) relations for a sequence of Bonnor–Ebert equilibrium states for constant external pressure $P_{\rm ext}$ (dashed line). Here, $R_0 = c_{\rm s}^2/(G^{1/2}P_{\rm ext}^{1/2})$ and $M_0 = c_{\rm s}^4/(G^{3/2}P_{\rm ext}^{1/2})$. The plotted sequence extends somewhat beyond the critical mass $M_{\rm crit} = 1.18\ M_0$. The dash–dotted line is the corresponding sequence for an external pressure $3\ P_{\rm ext}$. The solid line with arrows represents a possible evolutionary sequence of a condensation during mass accretion, terminating with collapse as the external pressure suddenly rises to a value incompatible with an equilibrium state.

For an exponential distribution of lifetimes, Reed derives an analytic four-parameter density function, more complicated than equation (7), but which also has the asymptotic dependence $f(m) \propto m^{-1-\alpha}$ for large m. We refer the reader to the above-mentioned papers for details.

While an exponential distribution of accretion termination times guarantees a power-law tail in the mass distribution, it is also true that all condensations need not *start* accreting at the same time. If the 'birth' of condensations is distributed uniformly in time throughout the life of a cloud, and termination times obey an exponential distribution, then the number of 'living' (i.e. still accreting) condensations at a fixed time t of observation will also obey an exponential distribution of times τ since birth, i.e. $f(\tau) = \delta\ \mathrm{e}^{-\delta\tau}$. Furthermore, if the 'birth' of condensations is also increasing exponentially in time with a growth rate β, then the distribution of times τ since birth will be $f(\tau) = (\beta + \delta)\ \mathrm{e}^{-(\beta+\delta)\tau}$. Hence observations of accreting condensations made at a single snapshot in time, e.g. Motte et al. (1998), should yield a power-law index $\alpha' = \alpha + \beta/\gamma$, so that the slope is equal to that of the IMF if $\beta = 0$ (or $\beta \ll \gamma$), but steeper otherwise.

3.2 A variation on the basic model

Accretional growth proportional to the instantaneous condensation mass is a plausible but unproven assumption. Myers (2000) used such a relation for the growth of condensations, but had to assume a very specific rate of growth of internal turbulence as accretion proceeded.

Here, we look at an alternative scenario, also based on Bonnor–Ebert spheres, but assuming that the internal velocity dispersion remains fixed during accretion. It is instructive to plot the radius versus mass (R–M) relation for the sequence of equilibrium states of increasing mass, but with fixed internal sound speed $c_{\rm s}$ and external pressure $P_{\rm ext}$. For small clouds, the R–M relation is found analytically from the Bonnor–Ebert theory (Bonnor 1956; Ebert 1957) to be

$$R = \left(\frac{3c_{\rm s}^2}{4\pi P_{\rm ext}}\right)^{1/3} M^{1/3}. \tag{8}$$

However, this approximation also yields radii that are within 20 per cent of the actual value for all $M/M_0 < 1$, where $M_0 = c_{\rm s}^4/(G^{3/2}P_{\rm ext}^{1/2})$ is the natural unit of mass in the Bonnor–Ebert problem. Fig. 3 shows the Bonnor–Ebert R–M sequence as well as the corresponding relationship for a higher external pressure $3P_{\rm ext}$.

In this simplified model, condensations start out somewhere on the equilibrium R–M sequence, increase their size R according to the curve as M grows by accretion, then make a jump downward after an ambient pressure fluctuation, as shown schematically by the solid line in Fig. 3. After the downward jump, no accessible equilibrium state may be present, and the condensation begins dynamical collapse.

If R exceeds the Bondi (1952) radius $R_{\rm B} \equiv GM/c_{\rm s,ext}$, where $c_{\rm s,ext}$ is the sound speed in the external medium, then a stationary condensation undergoes geometric accretion:

$$\frac{\mathrm{d}M}{\mathrm{d}t} = 4\pi R^2 \rho_{\rm ext} c_{\rm s,ext}. \tag{9}$$

Equations (8) and (9) then lead to

$$\frac{\mathrm{d}m}{\mathrm{d}t} = \gamma_1 m^{2/3} \ \Rightarrow\ m(t) = \left(m_0^{1/3} + \frac{\gamma_1}{3}t\right)^3, \tag{10}$$

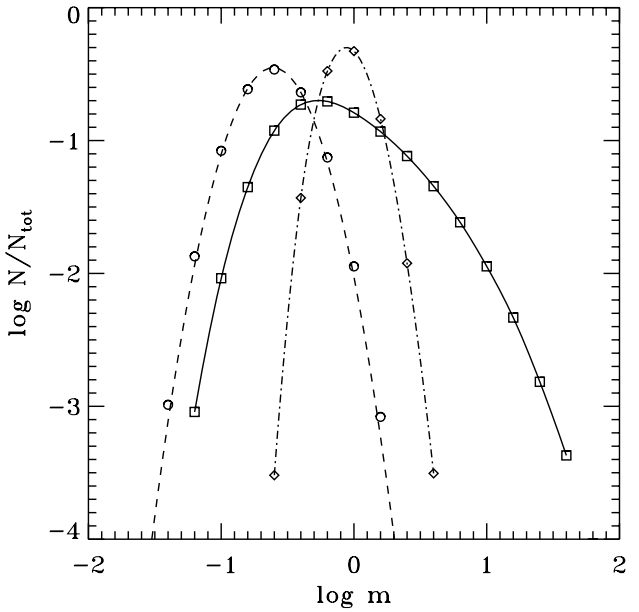

Figure 4. Evolution of a distribution of normalized masses m undergoing accretion growth $\mathrm{d}m/\mathrm{d}t \propto m^{2/3}$ (equation 10). The dashed line is an example of an initial lognormal distribution with $\mu_0 = -1.40$, $\sigma_0 = 0.52$. A sample of 10^6 masses drawn from this distribution is binned in increments Δ log $m = 0.2$ and represented by circles. The diamonds (connected by a dash–dotted line) are a histogram of masses after they have all accreted for a time $t = \gamma_1^{-1}$, and the squares (connected by a solid line) are a histogram of masses if the accretion lifetimes have density function $f(t) = \delta\, \mathrm{e}^{-\delta t}$, in which $\delta = \gamma_1$.

where $m = M/M_0$ is a normalized mass, m_0 is the initial normalized mass, and $\gamma_1 = (36\,\pi)^{1/3} t_\mathrm{d}^{-1} = 4.84\, t_\mathrm{d}^{-1}$ is a growth rate.

Fig. 4 shows the evolution of the probability density function $f(m)$ from an initial lognormal distribution (same as in Fig. 2) to a later distribution under the assumptions (1) that all condensations grow for a fixed time $t = \gamma_1^{-1}$, and (2) that condensations grow for times that are distributed exponentially, with 'death' rate $\delta = \gamma_1$. The first case leads to a profile that resembles a lognormal, but is narrower than the initial distribution, and the second case leads to a distinctly non-lognormal profile which may be described as a broken power law with two distinct regions; best-fitting slopes $\Gamma = \mathrm{d}\ \log\ N/\mathrm{d}\ \log\ m$ are equal to -1.0 in the intermediate-mass range ($1 \leqslant m < 10$), -2.4 in the high-mass range ($10 \leqslant m < 100$), and -1.6 for all $m \geqslant 1$. Interestingly, a broken power law with a steeper slope at high masses is reminiscent of some descriptions of the field star IMF (Kroupa & Weidner 2003).

4 CONCLUSIONS

We believe that the basic features of this model will be preserved in more complicated and realistic scenarios: that is, even a lognormal distribution of condensation masses at birth coupled with subsequent accretion growth (proportional to some power of mass) in which the accretion time obeys its own distribution (approximately exponential) will result in a power-law tail.

Zinnecker (1982) has presented another model of accretion growth in which a distribution of initial masses m_0 undergo Bondi accretion ($\dot{m} \propto m^2$); the exponent greater than 1 means that small differences in the m_0 values are magnified over time. After a fixed accretion time for all objects, when $m \gg m_0$, $f(m)$ tends to a power-law form with index -2. For comparison, the mechanism of exponential distribution of lifetimes studied in this paper yields a power-law tail even if the initial masses are all the same. The general combination of accretion growth (due to the Bondi process or geometric accretion) and a distribution of accretion lifetimes (where both processes are controlled by the dynamical time of the parent system) may play a role in determining the IMF in detailed global simulations of star formation (e.g. Bate, Bonnell & Bromm 2003) in which stars are formed throughout the duration of the simulation. Other ideas related to the *spatial* structure of turbulence may also contribute to power-law fragment masses, e.g. thresholded regions in density fields with lognormal probability density functions may have power-law clump mass distributions (Pudritz 2002; Elmegreen 2002). However, we believe that the *temporal* effect studied in this paper provides a compelling part of the explanation for the power-law tail in the IMF.

ACKNOWLEDGMENTS

SB was supported by a grant from the Natural Sciences and Engineering Research Council of Canada (NSERC). CEJ acknowledges an NSERC Postdoctoral Fellowship.

REFERENCES

Adams F. C., Fatuzzo M., 1996, ApJ, 464, 256
Bate M. R., Bonnell I. A., Bromm V., 2003, MNRAS, 339, 577
Bondi H., 1952, MNRAS, 112, 195
Bonnell I. A., Davies M. B., 1998, MNRAS, 295, 691
Bonnor W. B., 1956, MNRAS, 116, 351
Ebert R., 1957, Afz, 42, 263
Elmegreen B. G., 2001, in Montmerle T., André P., eds, ASP Conf. Ser. Vol. 243, From Darkness to Light. Astron. Soc. Pac., San Francisco, p. 255
Elmegreen B. G., 2002, ApJ, 564, 773
Hillenbrand L. A., 1997, AJ, 113, 1733 (H97)
Ioka K., Nakamura T., 2002, ApJ, 570, L21
Jeans J. H., 1928, Astronomy and Cosmogony. Cambridge Univ. Press, Cambridge
Johnstone D., Wilson C. D., Moriarty-Schieven G., Joncas G., Smith G., Gregersen E., Fich M., 2000, ApJ, 545, 327
Klessen R. S., 2001, ApJ, 556, 837
Kroupa P., Weidner C., 2003, ApJ, 598, 1076
Miller G. E., Scalo J. M., 1979, ApJS, 41, 513
Meyer M. R., Adams F. C., Hillenbrand L. A., Carpenter J. M., Larson R. B., 2000, in Mannings V., Boss A. P., Russell S. S., eds, Protostars and Planets IV. Univ. Arizona Press, Tucson, AZ, p. 121
Mitzenmacher M., 2004, Internet Mathematics, 1, 193
Motte F., André P., Neri R., 1998, A&A, 336, 150
Myers P. C., 2000, ApJ, 530, L119
Ostriker E. C., Stone J. M., Gammie C. F., 2001, ApJ, 546, 980
Padoan P., Nordlund A., Jones B. J. T., 1997, MNRAS, 288, 145
Pudritz R. E., 2002, Sci, 295, 68
Reed W. J., 2002, J. Regional Sci., 42, 1
Reed W. J., 2003, Phys. A, 319, 469
Reed W. J., Hughes B. D., 2002, Phys. Rev. E, 66, 7103
Salpeter E. E., 1955, ApJ, 121, 161
Scalo J., 1998, in Gilmore G., Howell D., eds, ASP Conf. Ser. Vol. 142, The Stellar Initial Mass Function. Astron. Soc. Pac., San Francisco, p. 201
Shu F. H., Allen A., Shang H., Ostriker E. C., Li Z.-Y., 1999, in Lada C. J., Kylafis N., eds, The Origin of Stars and Planetary Systems. Kluwer, Dordrecht, p. 193
Testi L., Sargent A. I., 1998, ApJ, 508, L91
Zinnecker H., 1982, in Glassgold A. E., Huggins P. J., Schucking E. L., eds, Symposium on the Orion Nebula to Honour Henry Draper. New York Acad. Sci., New York, p. 226

This paper has been typeset from a TEX/LATEX file prepared by the author.